Electronic Supplementary Material (ESI) for Chemical Science

Insight into the Construction of Metal–Organic Polyhedra: Metal–Organic Cubes as a Case Study

Mohamed H. Alkordi,[†,‡] Jonathan L. Belof,[†] Edwin Rivera,[†] Lukasz Wojtas,[†] and Mohamed Eddaoudi*[†,‡]

[†]*Department of Chemistry, University of South Florida, Tampa, Florida 33620-5250*

[‡]*Advanced Membranes and Porous Materials Center, 4700 King Abdullah University of Science and Technology (KAUST), Thuwal, KSA*

Mohamed.Eddaoudi@kaust.edu.sa

Experimental Details:

NMR measurements. All 1H and 13C NMR spectra were acquired on Varian VXR (299.94 MHz for ^{1}H, 75.55 MHz for ^{13}C), UnityINOVA 400 (399.78 MHz for ^{1}H, 100.54 MHz for ^{13}C) equipped with Performa I single axis gradient Z amplifier and a Varian 5mm auto switchable Z gradient probe and variable temperature controller, or UnityINOVA 500 (499.76 MHz for ^{1}H, 125.68 MHz for ^{13}C) equipped with a Performa II single axis Z gradient amplifier and a Varian 5mm Triple Resonance Z gradient probe spectrometers. The ^{1}H chemical shifts are reported relative to that of TMS and referenced to either the internal HDO signal at 4.76 ppm, the singlet peak of 3-(trimethylsilyl)-1-propanesulfonic acid sodium salt (DSS) at 0 ppm, or DMSO-d6 signal at 2.5 ppm, as indicated for each spectrum. Variable temperature measurements were conducted on a sample of **1** dissolved in D_2O and held at the specific temperature for 10 min prior to spectrum acquisition. Solution ^{1}H NMR measurements at variable pH were conducted at 296 K on a mixture prepared by mixing $CoCl_2$ (1 mmol, 0.066 M) and H-**L1** (1.5 mmol, 0.1 M) in 15 mL of D_2O (resulted pH = 6.63), stirred under aerobic conditions at 296 K for 1 h prior to pH adjustments. The pH is adjusted through incremental additions of either NaOD or D_2SO_4, as required, and the apparent solution pH values are reported. Measurements are made with Mettler Toledo EL02 pH meter calibrated with aqueous buffer solutions at 296 K.

Spectrophotometric titration. 15 solutions containing $CoCl_2$ (20 mL, 2.5 mM, 0.05 mmol) and increasing amounts of H-L1 (0.01-0.15 mmol, 0.01 mmol increment) were prepared. The pH values for each solution were measured at different time intervals. The mixtures were incubated at 296 K for 24 h, under atmospheric conditions, before conducting absorbance measurements at 493 nm.

Single-Crystal X-ray Diffraction. X-ray diffraction data were collected using Bruker-AXS SMART-APEX CCD diffractometer equipped with Mo Kα radiation source (λ = 0.71073 Å) or SMART-APEX CCDII diffractometer equipped with Cu Kα (λ = 1.54178 Å) radiation source, as indicated. Indexing was performed using SMART v5.625.[1] Frames were integrated with SaintPlus 6.28A [2] software package. Absorption correction was performed by multi-scan method implemented in SADABS.[3] Crystal structures were solved using SHELXS-97 and refined using SHELXL-97 contained in SHELXTL v6.10 and WinGX v1.70.01 programs packages.[4] All non-disordered non-hydrogen atoms were refined with anisotropic displacement parameters. All H-atoms bonded to carbon atoms were placed in geometrically optimized positions and refined with an isotropic displacement parameter fixed at 1.2 times Uq. N bonded protons were localized via Fourier difference map inspection and refined isotropically with thermal parameters, based on the N atoms to which they are bonded.

Other Physical Measurements. Powder X-ray diffraction (XRPD) data were collected using Cu Kα radiation (λ = 1.5406Å) on a Bruker AXS D8−Advance diffractometer. The MALDI−TOF MS spectrum was recorded on a Bruker Daltonics Autoflex III TOF/TOF mass spectrometer using α-cyanohydroxy-cinnamic acid as the matrix. Solution UV–vis absorption spectra were collected on a PerkinElmer Lambda 900 spectrophotometer, with an attachment for solid samples and gaseous atmosphere. Stopped-flow kinetics data are collected on a Bio-Logic instrument (SFM300 mixer and MOS200M monochromator) and the data were fitted with Origin®.

Computer Modelling. The hydrated fragment $[Co_2(L1)(H_2O)_8]^{3+}$, with a +3 net charge and multiplicity of 7, was geometry optimized using the quantum chemistry code Gaussian 03.5 The minimized energy was calculated via Density Functional Theory (DFT) using the B3LYP hybrid exchange-correlation functional.[6] The unrestricted calculation employed the LANL2DZ basis set with an ECP applied to the cobalt atoms.[7]

Synthetic procedures for compounds 1(a-f) and 2-4:

$[Co_8(C_{11}N_6H_{15})_{12}]Br_{12}\cdot 18H_2O$, 1a. In a capped 25 mL scintillation vial, reaction of H-**L1** (0.034 g, 0.15 mmol) and $CoBr_2\cdot 6H_2O$ (0.0325 g, 0.1 mmol) in a mixture of DMF and water, 1 mL each, at 115°C for 12 h resulted in red polyhedral crystals (0.051 g, 90 % yield based on $CoBr_2$) formulated as $[Co_8(C_{11}N_6H_{15})_{12}]Br_{12}\cdot 18H_2O$, from single-crystal X-ray diffraction.

$[Co_8(C_{11}N_6H_{15})_{12}](SO_4)_6\cdot(DMF)\cdot 31H_2O$, 1b. In a capped 25 mL vial, reaction of H-**L1** (0.034 g, 0.15 mmol) and $Co(SO_4)\cdot 6H_2O$ (0.0263 g, 0.1 mmol) in a mixture of DMF and water, 1 mL each, at 115°C for 12 h resulted in red polyhedral crystals (0.023 g, 41.3% yield based on $Co(SO_4)$) formulated as $[Co_8(C_{11}N_6H_{15})_{12}](SO_4)_6(DMF)\cdot 31H_2O$, from single-crystal X-ray diffraction.

$[Co_8(C_{11}N_6H_{15})_{12}][CoCl_4]_2Cl_8\cdot 21H_2O$, 1c. In a capped 25 mL scintillation vial, reaction of H-**L1** (0.034 g, 0.15 mmol) and $CoCl_2\cdot 6H_2O$ (0.0237 g, 0.1 mmol) in a mixture of dimethylsulfoxide (DMSO) and water, 1 mL each, at 115°C for 24 h resulted in brown rectangular crystals (0.01 g, 23% yield based on $CoCl_2$), formulated as $[Co_8(C_{11}N_6H_{15})_{12}]$ $[CoCl_4]_2Cl_8\cdot 21H_2O$, from single crystal X-ray diffraction.

$[Co_8(C_{11}N_6H_{15})_{12}](NO_3)_{12}\cdot 22H_2O$, 1d. In an open 25 mL scintillation vial, a mixture of H-**L1** (0.034 g, 0.15 mmol) and $Co(NO_3)_2\cdot 6H_2O$ (0.1 mmol) in *N,N`*-diethylformamide (DEF) and water, 1 mL each, was prepared and left to stand at r.t. After seven days the reaction volume was reduced to almost 1 mL through evaporation and red crystals were collected (0.038 g, 70.2% yield based on $Co(NO_3)_2$), formulated as $[Co_8(C_{11}N_6H_{15})_{12}](NO_3)_{12}\cdot 22H_2O$ from single crystal X-ray diffraction.

$[Co_8(C_{11}N_6H_{15})_{12}](BF_4)_{12}\cdot 2(DMF)\bullet 14H_2O$, 1e. In a capped 25 mL scintillation vial, reaction of H-**L1** (0.034 g, 0.15 mmol) and $Co(BF_4)_2\cdot 6H_2O$ (0.1 mmol) in a mixture of DMF and water, 1 mL each, at115°C for 12 h resulted in red polyhedral crystals (0.04 g, 68.2% yield based on $Co(BF_4)_2$) formulated as $[Co_8(C_{11}N_6H_{15})_{12}](BF_4)_{12}\cdot 2(DMF)\cdot 14H_2O$, from single-crystal X-ray diffraction.

$[Co_8(C_{11}N_6H_{15})_{12}]Cl_{12}\cdot 40H_2O$, 1f. In a capped 25 mL scintillation vial, reaction of H-**L1** (0.034 g, 0.15 mmol) and $CoCl_2\cdot 6H_2O$ (0.1 mmol) in a mixture of hexamethylphosphoramide (HMPA) and water, 1 mL each, at115°C for 12 h resulted in red polyhedral crystals (0.035 g, 63.7% yield based on $CoCl_2$) formulated as $[Co_8(C_{11}N_6H_{15})_{12}]Cl_{12}\cdot 40H_2O$ using single-crystal X-ray diffraction.

$[Ni_4(C_{11}N_6H_{15})_4](NO_3)_4(DMF)_4$, 2. In a capped 25 mL scintillation vial, reaction of H-**L1** (0.023 g, 0.1 mmol) and $Ni(NO_3)_2\cdot 6H_2O$ (0.1 mmol) in 1 mL of DMF at room temperature for 12 h, resulted in green-blue polyhedral crystals (0.006 g, 14 % yield based on $Ni(NO_3)_2$) formulated as $[Ni_4(C_{11}N_6H_{15})_4](NO_3)_4(DMF)_4$ using single crystal X-ray diffraction.

$[Cd(C_{11}N_6H_{15})(NO_3)]_n$, 3. In a capped 25 mL scintillation vial, reaction of H-**L1** (0.023 g, 0.1 mmol) and $Cd(NO_3)_2\cdot 4H_2O$ (0.1 mmol) in 1 mL of DMF at 85°C for 12 h, resulted in colorless polyhedral crystals (0.017 g, 42 % yield based on $Cd(NO_3)_2$) formulated as $[Cd(C_{11}N_6H_{15})(NO_3)]_n$ using single crystal X-ray diffraction.

$[In_8(C_{11}N_6H_{15})_{12}](NO_3)_{12}\cdot 4H_2O$, 4. In a capped 25 mL scintillation vial, reaction of H-**L1** (0.034 g, 0.15 mmol) and $In(NO_3)_3\cdot 5H_2O$ (0.1 mmol) in DEF (5 mL) and ethanol (2 mL) at 85°C for 12 h, resulted in colorless polyhedral crystals (0.0225 g, 40% yield based on $In(NO_3)_3$) formulated as $[In_8(C_{11}N_6H_{15})_{12}](NO_3)_{12}\cdot 4H_2O$ using crystal X-ray diffraction.

Crystallographic data table:

Table S1. Crystallographic data for **1-4** and **1(a-f)**.

	1	**2**	**3**	**4**	**1a**
Formula	$C_{132}H_{180}N_{72}O_4Co_8Cl_{12}$	$C_{56}H_{88}N_{32}Ni_4$	$C_{14}H_{22}N_8O_4Cd$	$C_{132}H_{126}N_{84}O_{40}In_8$	$C_{132}H_{156}N_{72}O_{18}Co_8Br_{12}$
Fwt, Z	3729.96, 4	1700.42, 4	478.80, 4	4442.39, 3	4469.65, 2
Crystal system	cubic	orthorhombic	monoclinic	trigonal	monoclinic
Space group	*P*a-3	*Pbca*	$P2_1/n$	*R*-3	$P2_1/n$
a, Å	25.1026(13)	17.3775(12)	12.909(2)	28.1055(4)	17.758(5)
b, Å	25.1026(13)	17.4940(12)	12.0710(19)	28.1055(4)	19.380(3)
c, Å	25.1026(13)	24.6892(17)	12.950(2)	19.1669(6)	24.772(6)
α°	90	90	90	90	90
β°	90	90	115.858(2)	90	90.257(16)
γ°	90	90	90	120	90
Wavelength, Å	0.71073	1.54178	0.71073	1.54178	1.54178
T, K	100(2)	100(2)	100(2)	100(2)	293(2)
Final R indices, [I>2σ(I)]	R1 = 0.0493, wR2 = 0.1350	R1 = 0.0702, wR2 = 0.1688	R1 = 0.0401, wR2 = 0.0966	R1 = 0.0577, wR2 = 0.1351	R1 = 0.0826, wR2 = 0.2615
GOF on F^2	1.026	1.005	1.052	1.031	0.975
	1b	**1c**	**1d**	**1e**	**1f**
Formula	$C_{135}H_{175}N_{73}O_{56}S_6Co_8$	$C_{138}H_{156}N_{72}O_8S_3Co_{10}Cl_{16}$	$C_{132}H_{156}N_{84}O_{59}Co_8$	$C_{138}H_{178}N_{74}O_{16}B_{12}Co_8F_{48}$	$C_{132}H_{168}N_{72}O_{40}Co_8Cl_{12}$
Fwt, Z	4380.28, 2	4260.03, 2	4326.85, 2	4654.7, 4	4300.22, 4
Crystal system	monoclinic	monoclinic	monoclinic	monoclinic	monoclinic
Space group	$P2_1/n$	*C*2/*m*	$P2_1/n$	*C*2/*c*	*C*2/*c*
a, Å	20.3067(9)	28.550(2)	20.155(5)	31.693(3)	33.008(8)
b, Å	18.7195(8)	22.5268(19)	19.422(5)	20.047(4)	19.253(5)
c, Å	24.9104(10)	19.4189(16)	22.792(6)	32.309(6)	32.654(7)
α°	90	90	90	90	90
β°	93.1820(10)	131.977(3)	90.221(2)	109.50(3)	116.116(5)
γ°	90	90	90	90	90
Wavelength, Å	1.54178	1.54178	1.54178	1.54180	1.54180
T, K	100(2)	293(2)	293(2)	100(2)	100(2)
Final R indices [I>2σ(I)]	R1 = 0.0737, wR2 = 0.1794	R1 = 0.0833, wR2 = 0.2286	R1 = 0.0782, wR2 = 0.1921	0.0789, wR2 = 0.1715	0.0714, wR2 = 0.1662
GOF on F^2	1.025	1.038	1.041	0.942	1.022

Relaxation times table:

Table S2. Experimental spin−lattice relaxation times (T_1) for ^{1}H signals (in the 7-24 ppm chemical shift range) of the paramagnetic reaction mixture, the corresponding cobalt-to-proton (r_{Co-H}) distances relative to the reference distance of 5.324 Å for the proton at δ = 8.68 ppm, and the r_{Co-H} distances obtained from the geometrically-optimized model of $[Co_2(\mathbf{L1})(H_2O)_8]^{3+}$ fragment.

Chemical Shift δ (ppm)	***T1* (s)**	**r_{Co-H} (experimental)**	**r_{Co-H} (model)**
7.652	0.1051	5.683	5.953
8.68	0.0710	5.324	5.324
9.319	0.1226	5.831	5.890
10.168	0.0859	5.495	5.345
10.608	0.0854	5.490	5.452
12.763	0.0217	4.370	4.506
13.452	0.0455	4.943	5.285
17.105	0.0240	4.443	4.742
21.969	0.0047	3.386	3.499
23.546	0.0103	3.858	3.692

Crystal structure description for compounds 1(a-f), and 2-4:

Single Crystal X-ray Structure Analysis of 1a, $[Co_8(C_{11}N_6H_{15})_{12}]Br_{12}\cdot 18H_2O$. In the crystal structure of **1a**, the cationic MOCs crystallize in the monoclinic $P2_1/n$ space group where the charge is balanced by twelve bromide counterions. Six bromide counterions decorate the faces of a MOC where hydrogen bond interactions between bromide ions and the pyrrole-type nitrogen atoms are present (N1`···Br distances of 3.0−3.394 Å), in a similar manner observed in **1**. One bromide ion occupies the cavity inside the MOC and the remaining five bromide ions are geometrically disordered over several positions. The aliphatic carbon atoms C5` are geometrically disordered. The Co–N bond lengths, 1.916−1.986 Å (*thp*) and 1.841−1.907 Å (imidazolate), are similar to those observed in **1**. On each of the six faces of a MOC, two parallel imidazolate rings are separated by centroid-to-centroid distances of 5.627−5.697 Å

Single Crystal X-ray Structure Analysis of 1b, $[Co_8(C_{11}N_6H_{15})_{12}](SO_4)_6\cdot(DMF)\cdot 31H_2O$. MOCs in **1b** crystallize in the monoclinic, $P2_1/n$ space group where each face of a MOC is decorated by a sulfate counterion, H-bonded to N1` atoms of *thp* rings. Each sulfate counterion is hydrogen bonded through two oxygen atoms to four N1` (N1`···O–S distances of 2.824−3.057 Å). Such multiple interactions between each sulfate ion and the N1` atoms appear to cause a noticeable decrease in the centroid-to-centroid distance (5.375−5.408 Å) between the two parallel imidazolate rings on each of the six faces of the MOC, shorter than those observed in **1** and **1a** for chloride (5.505 Å) and bromide (5.627−5.697 Å) counterions, respectively. The Co–N bond lengths of 1.917−1.994 Å (*thp*), and 1.89−1.895 Å (imidazolate), closely matches those observed in **1** and **1a**.

Single Crystal X-ray Structure Analysis of 1c, $[Co_8(C_{11}N_6H_{15})_{12}][CoCl_4]_2Cl_8\cdot 21H_2O$. In **1c**, discrete MOCs crystallize in the monoclinic *C2/m* space group. Each MOC cocrystallize with two $[CoCl_4]^{2-}$ anions involved in hydrogen bond interactions to adjacent MOC (C−H···Cl distances of 2.608−2.935Å, normalized data). Charge balance is satisfied by eight chloride counterions. One chloride counterion occupies the cavity inside the MOC. The additional seven Cl^- ions, geometrically disordered over multiple positions adjacent to the faces of the MOC, are H-bonded to the N1` atoms on each of the faces of the MOC (N···Cl distances of 3.21−3.615 Å). In the MOC, Co–N bond lengths of 1.945−1.953 Å (*thp*) and 1.88−1.901 Å (imidazolate) are in close agreement with those observed in compounds **1-1b**. On each of the six faces of a MOC, two parallel imidazolate rings are separated by centroid-to-centroid distances of 5.569−5.58 Å.

Single Crystal X-ray Structure Analysis of 1d, $[Co_8(C_{11}N_6H_{15})_{12}](NO_3)_{12}\cdot 22H_2O$. The cationic MOCs in **1d** crystallize in the $P2_1/n$ space group and the charge is balanced by twelve disordered nitrate counterions. One nitrate ion occupies the cavity inside the MOC and is hydrogen bonded to the C2 hydrogen atoms of the imidazolate rings, (C···O distances of 2.268−2.901 Å). The remaining nitrates ions are hydrogen bonded to the N1` atoms of the ligand molecules, decorating the faces (N···O distances of 2.903−3.067 Å) and the edges (N···O distances of 2.894−2.981 Å) of the MOC. In the crystal structure of **1d**, the MOCs are held together through bridging, hydrogen bonded, nitrate counterions. In the MOC, Co–N bond lengths of 1.932−1.95 Å (*thp*) and 1.899−1.921 Å (imidazolate) are in close agreement with those observed in compounds **1**-**1c**. On each of the six faces of a MOC, two parallel imidazolate rings are separated by centroid-to-centroid distances of 5.623−5.69 Å.

Single Crystal X-ray Structure Analysis of 1e, $[Co_8(C_{11}N_6H_{15})_{12}](BF_4)_{12}\cdot 2(DMF)\cdot 14H_2O$. The cationic MOCs in **1e** crystallize in the $C2/c$ space group where the charge is balanced by twelve $(BF_4)^-$ counterions. One disordered $(BF_4)^-$ ion occupies the cavity inside the MOC while the remaining disordered $(BF_4)^-$ ions are hydrogen bonded to the N1` atoms of the ligand molecules, decorating the faces and edges of the MOC. In the crystal structure of **1e**, the MOCs are held together through bridging, hydrogen bonded, $(BF_4)^-$ counterions. In the MOC, Co–N bond lengths of 1.937−1.940 Å (*thp*) and 1.896−1.918 Å (imidazolate) are in close agreement with those observed in compounds **1**-**1d**. In **1e**, each MOC cocrystallize with two DMF solvent molecules hydrogen bonded to two faces of the MOC, (N···O distances of 2.806−2.849 Å). On each of the six faces of a MOC, two parallel imidazolate rings are separated by centroid-to-centroid distances of 5.631−5.672 Å.

Single Crystal X-ray Structure Analysis of 1f, $[Co_8(C_{11}N_6H_{15})_{12}]Cl_{12}\cdot 40H_2O$. The cationic MOCs in **1f** crystallize in the $C2/c$ space group where the charge is balanced by twelve chloride counterions. One chloride ion occupies the cavity inside the MOC. The remaining chloride ions are hydrogen bonded to the N1` atoms of the ligand molecules, decorating the faces (N···Cl distances of 3.139−3.231 Å) and the edges (N···Cl distances of 2.888−3.141 Å) of the MOC. In the crystal structure of **1f**, the MOCs are held together through bridging, hydrogen bonded, water molecules. In the MOC, Co–N bond lengths of 1.937−1.956 Å (*thp*) and 1.895−1.909 Å (imidazolate) are in close agreement with those observed in compounds **1**-**1e**. On each of the six faces of a MOC, two parallel imidazolate rings are separated by centroid-to-centroid distances of 5.641−5.661 Å.

Single Crystal X-ray Structure Analysis of 2, $[Ni_4(C_{11}N_6H_{15})_4](NO_3)_4 \cdot 4(DMF)$. In the crystal structure of **2**, each Ni(II) ion is coordinated to one nitrate ion in bidentate fashion and two ligands **L1,** *cis*-MN_4O_2. Each neutral molecular square crystallizes with four DMF solvent molecules. The four ligand molecules, forming molecular squares, are hydrogen bonded through N1` atoms to four DMF molecules (N···O distances of 2.897−2.99 Å). Intramolecular H-bonds between the two *thp* rings of the molecular square are present (N−H···N distances of 2.279−2.289 Å). Ni–N bond lengths are in the range of 2.033−2.073 Å (*thp*) and 2.023−2.045 Å (imidazolate).

Single Crystal X-ray Structure Analysis of 3, $[Cd(C_{11}N_6H_{15})(NO_3)]_n$. The extended structure, chain, in **3** result from coordination of mono-deprotonated **L1** and Cd(II) ions, distorted octahedral *cis*-MN_4O_2. Each ligand in the chains is H-bonded to one DMF molecule and to a nitrate ion from the adjacent chain. Furthermore, intramolecular H-bonds exist between the sp^3-type N1` atoms (N−H···N distances of 2.377−2.610 Å). In **3**, Cd– N bond lengths of 2.231−2.269 Å (*thp*) and 2.311−2.374 Å (imidazolate) are observed.

Single Crystal X-ray Structure Analysis of 4, $[In_8(C_{11}N_6H_{15})_{12}](NO_3)_{12} \cdot 4H_2O$. The cationic MOCs in **4** crystallize in the *R*-3 space group where the charge is balanced by twelve nitrate counterions. One nitrate ion occupies the cavity inside the MOC. Six nitrates ions are hydrogen bonded to the N1` atoms of the ligand molecules on the faces of the MOC (N···O distances of 2.706−3.032 Å). The other five nitrate ions are geometrically disordered over several positions. In the MOC, the In–N bond lengths are in the range of 2.176−2.25 Å (*thp*) and 2.203−2.223 Å (imidazolate). On each of the six faces of a MOC, the centroid-to-centroid distance between two parallel imidazolate rings is 6.465 Å.

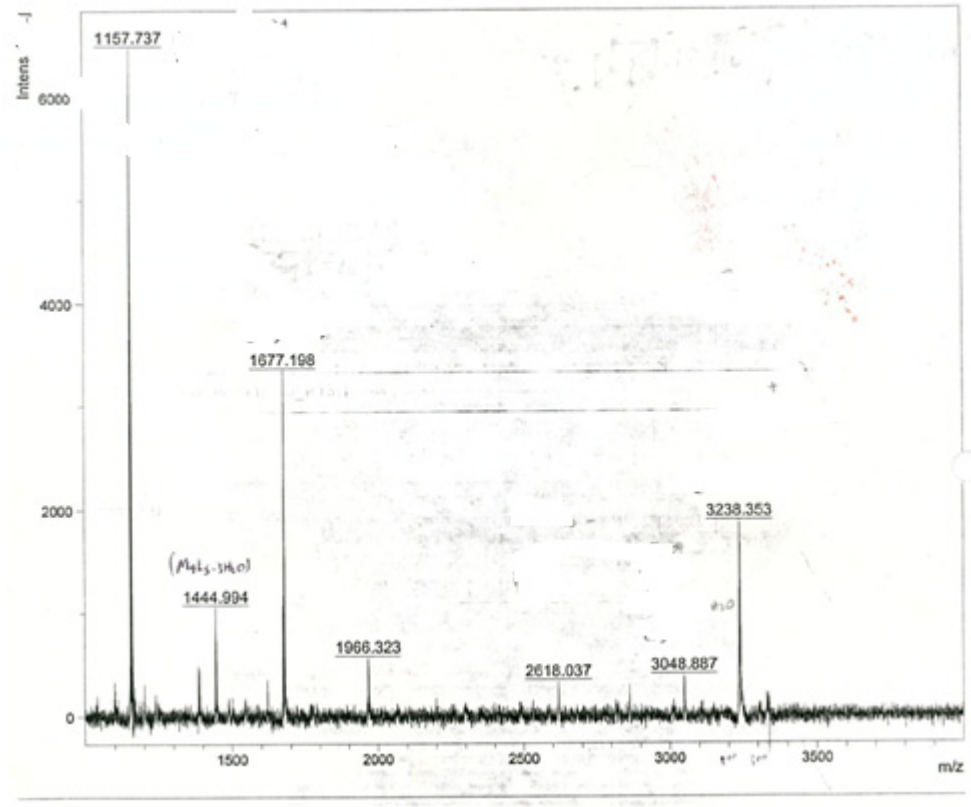

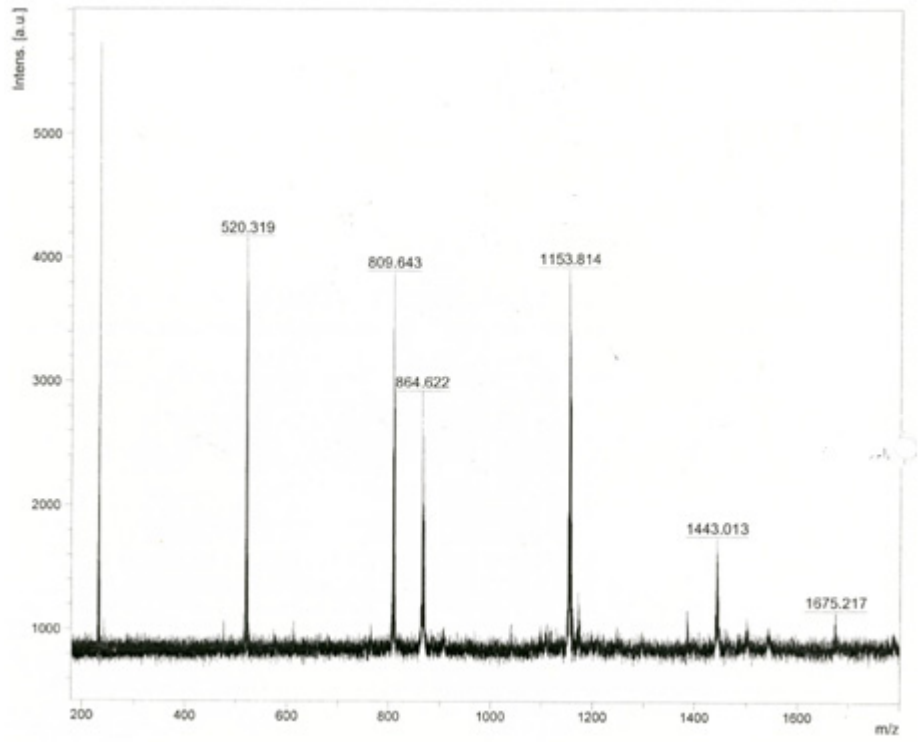

Figure S1. MALDI-TOF MS spectra for **1.**

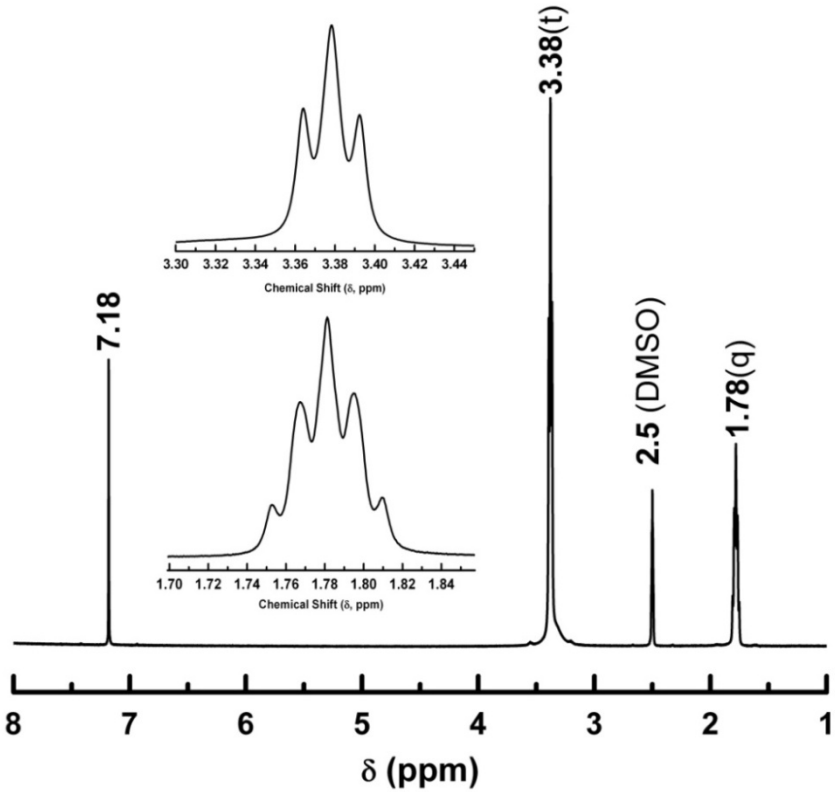

Figure S2. ^{1}H NMR spectrum of **L1** in DMSO-d_6.

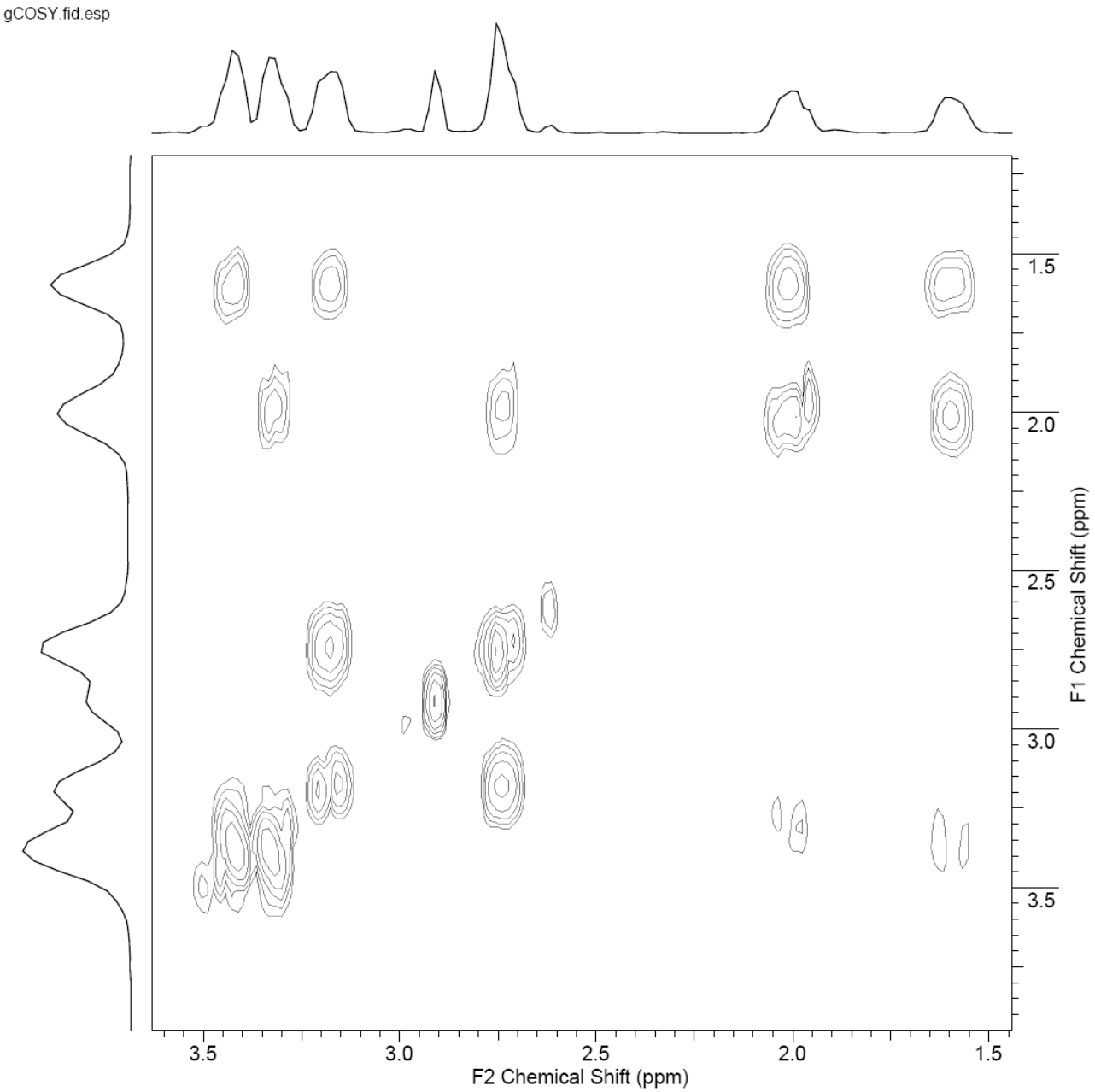

Figure S3. ^{1}H-{^{1}H} gCOSY spectrum for 1S in D2O. Peak at 2.9 ppm and side band at 2.71 ppm are assigned for residual DMF solvent molecules from the reaction mixture.

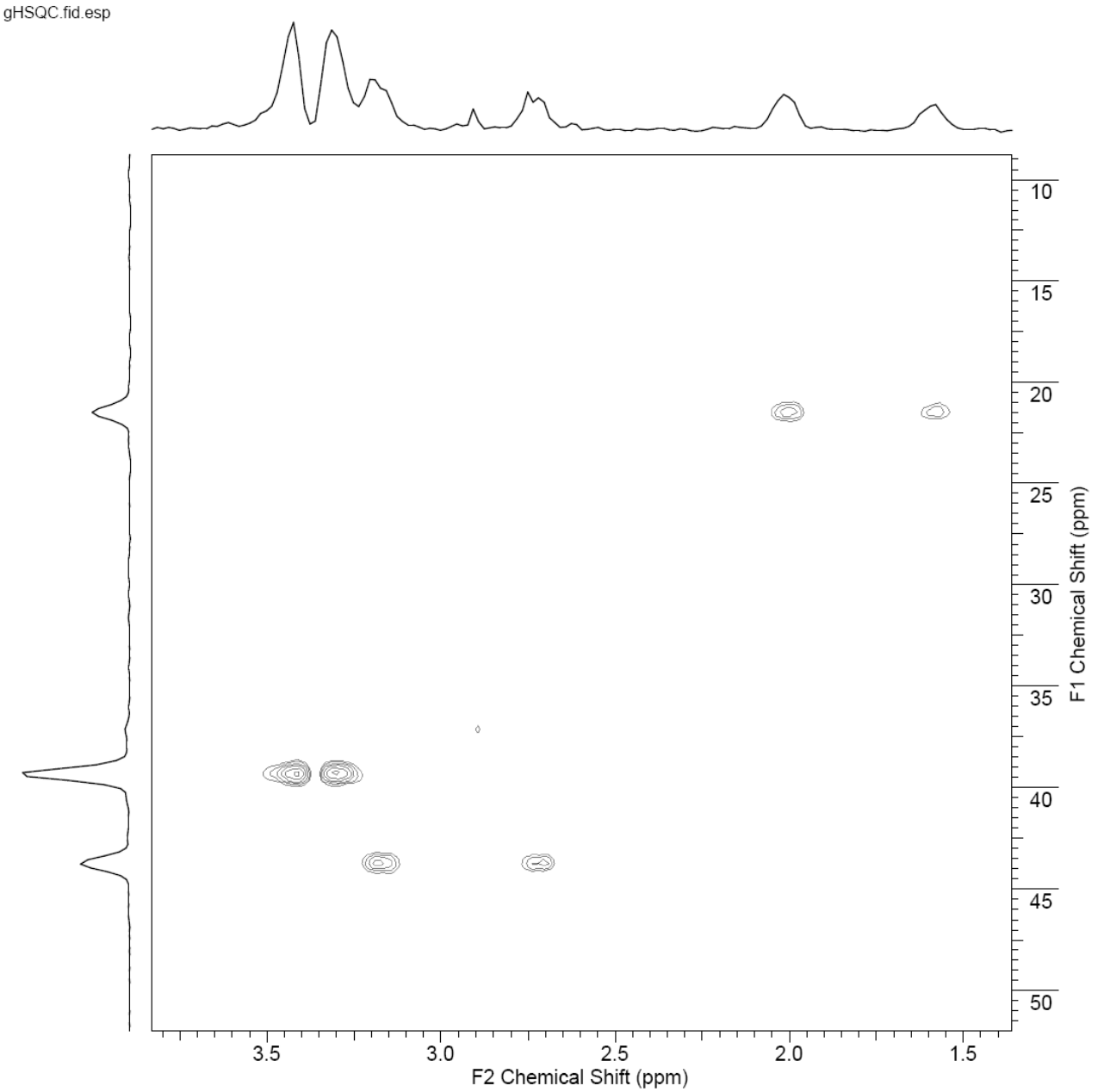

Figure S4. ^{1}H-{^{13}C} gHSQC spectrum for **1S** in D_2O.

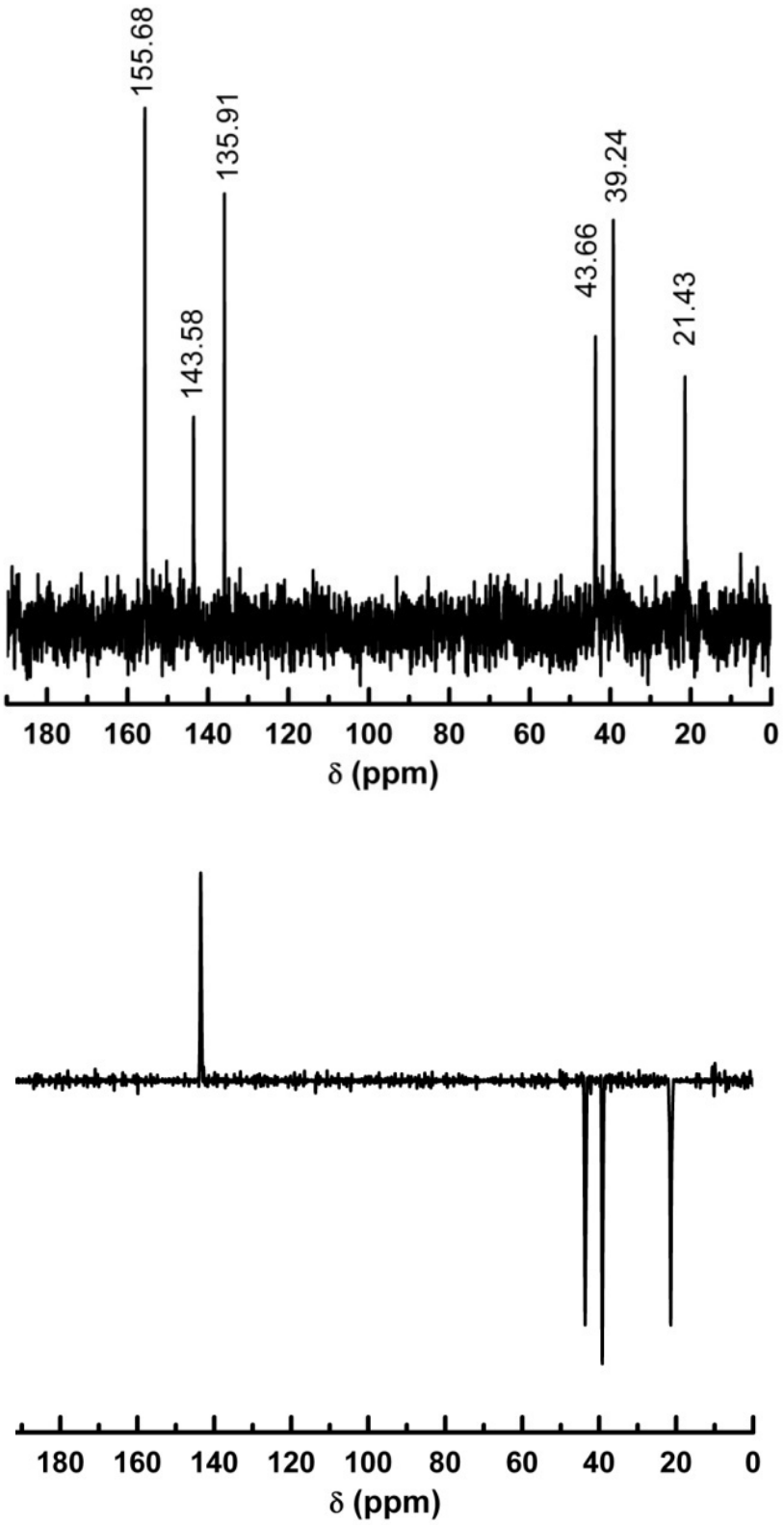

Figure S5. (Above) ^{13}C NMR spectrum of **1S** in D_2O. Peaks at 39.21 ppm and 43.65 ppm indicate different chemical shifts for C(4) and C(6) carbon atoms of *thp* rings, respectively, due to chelation of **L1** to cobalt ions. (Below) ^{13}C DEPT135º spectrum of **1S** in D_2O.

```
exp4  Dbppste_cc

      SAMPLE              FLAGS          ACQUISITION ARRAYS
date   Sep 30 2009  triax_flg        n  array         gzlvl1
solvent        d2o  il               n  arraydim         15
file           exp  in               n
   ACQUISITION      dp               y   i           gzlvl1
sfrq       499.765  alt_grd          n   1             1000
tn              H1  lkgate_flg       n   2             7499
at           2.000  sspul            y   3            10558
np           38462  satmode        nnn   4            12911
sw          9615.4      2D DISPLAY       5            14898
fb            5000  sp1            0.1   6            16649
bs              16  wp1            4.1   7            18232
ss              -4  sc2              0   8            19689
tpwr            56  wc2            155   9            21045
pw             8.0  rfl1          18.9  10            22318
d1           1.000  rfp1          18.9  11            23523
tof          599.5      DEC. & VT       12            24669
nt             256  dn              C13  13            25765
ct             256  dof               0  14            26815
gain            30  dm              nnn  15            27826
delflag          y  dmm               c
del         0.1000  dmf           32258
del2             0  dpwr             42
gzlvl1     arrayed  temp          25.0
gt1         0.0040      PROCESSING
kappa        0.150  lb             2.00
gstab       0.0003  proc             ft
gzlvl2         4393  fn            16384
gt2         0.0030  math              f
gzlvl3         6589    2D PROCESSING
gt3         0.0030  lb1            0.32
gzlvlhs        7138  proc1            ft
hsgt        0.0010  fn1             512
calibflag         n       DISPLAY
dosytimecubed 0.00~ sp            639.4
     0001519957000  wp           2426.1
dosyfreq undefined  vs            16350
DAC_to_G 0.0021323  sc                6
satdly        2.000  wc              225
satpwr            0  hzmm          13.38
satfrq        599.5  is            145.35
  2D ACQUISITION     rfl           1709.3
sw1           20.8  rfp                0
ni             256  th                 0
                    ins            1.000
                    a1    ph
```

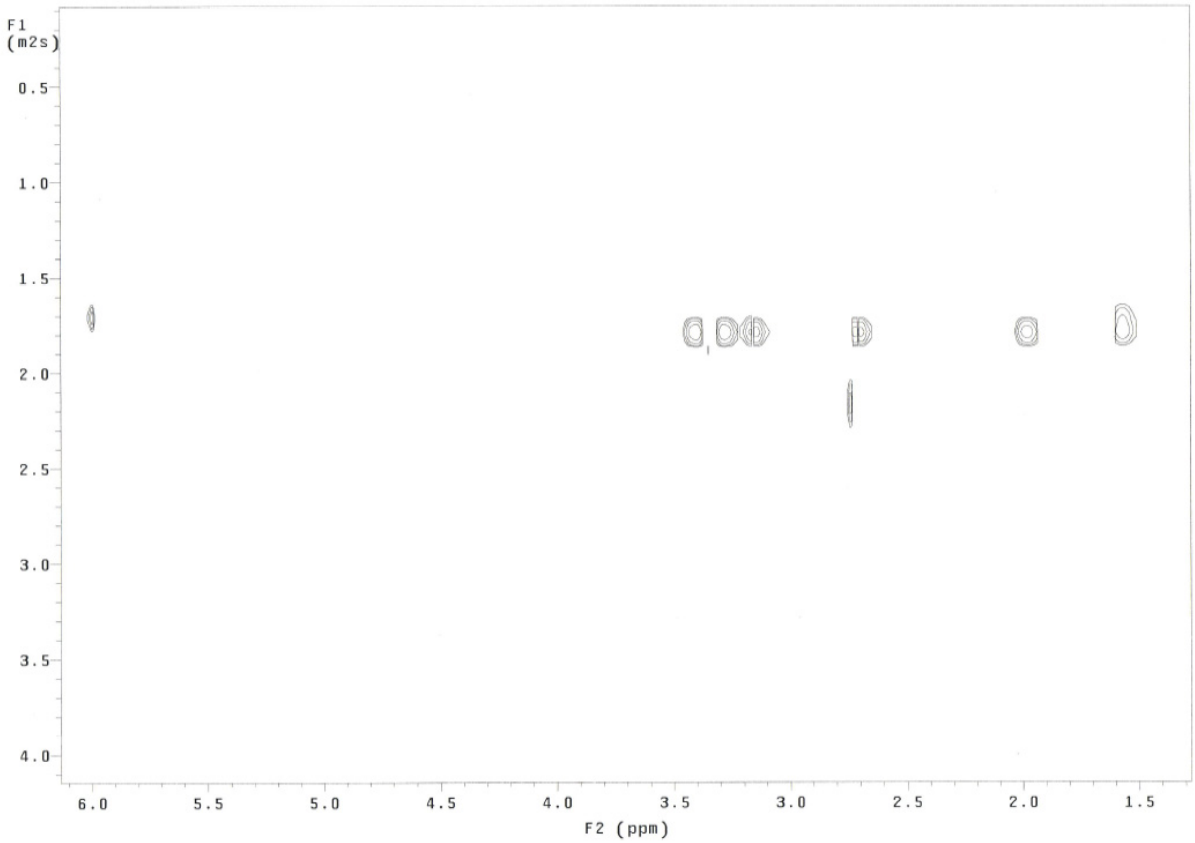

Figure S6. ^{1}H 2D-DOSY spectrum for 1S, 1.2 mM in D_2O at 298 K.

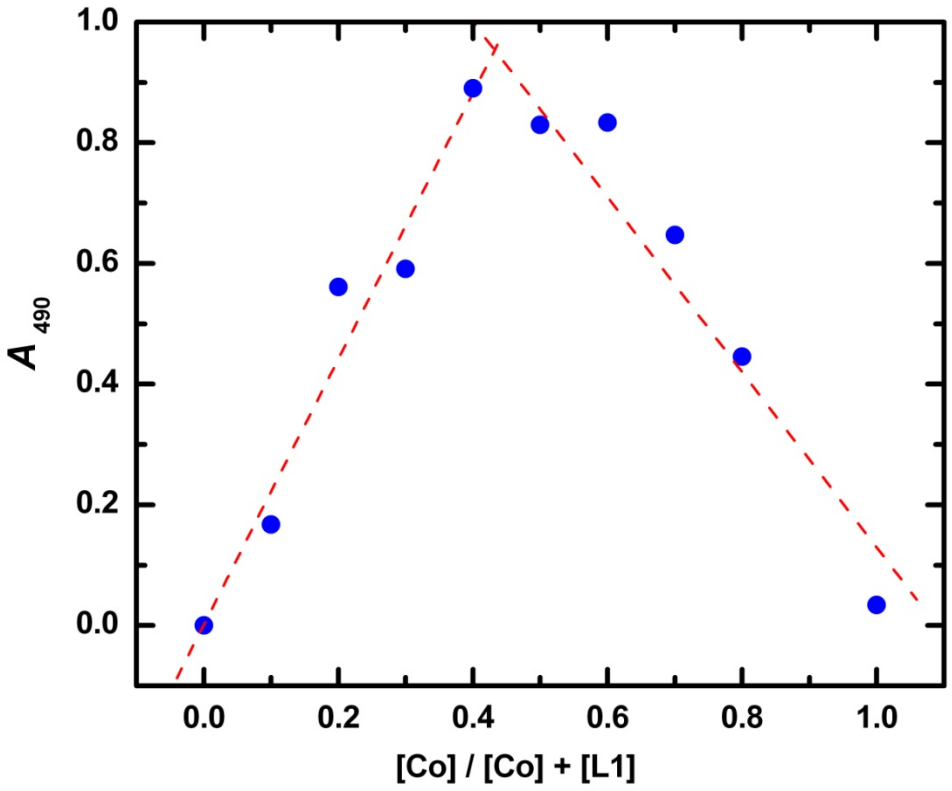

Figure S7. Job plot for the two binding species, $CoCl_2$ and H-**L1** in aqueous solution. Maximum absorbance reached at 0.4 mole fraction of Co ions, corresponding to 1.5:1 (ligand-to-cobalt) stoichiometry.

❖ Figures **S8-S13** are NMR spectra for the reaction mixture of $CoCl_2 \cdot 6H2O$ (0.1 mmol), H-**L1** (0.3 mmol), and $NaOCH_3$ (0.3 mmol) in 1 mL D_2O under aerobic conditions after standing at r.t. for 24 h.

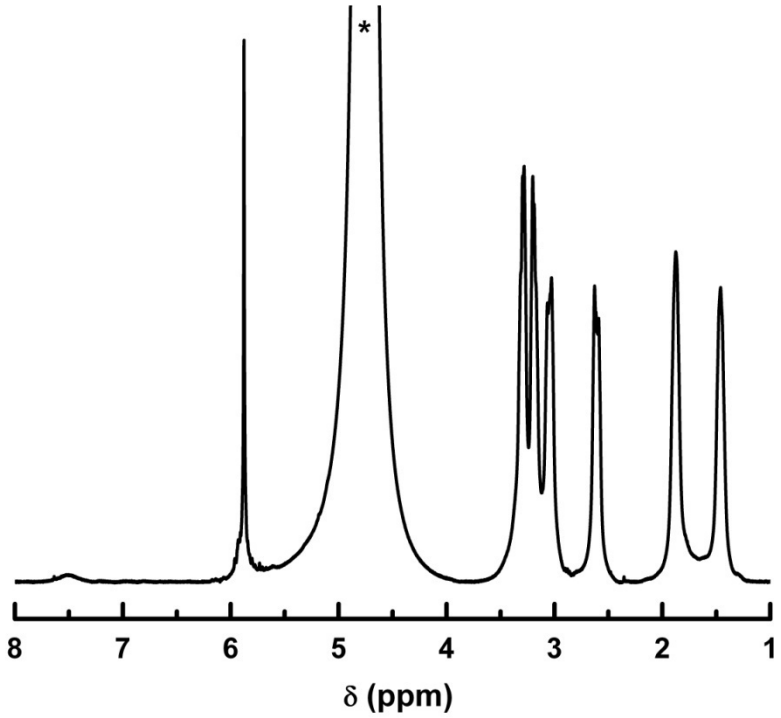

Figure S8. The ^{1}H NMR spectrum for the reaction mixture.

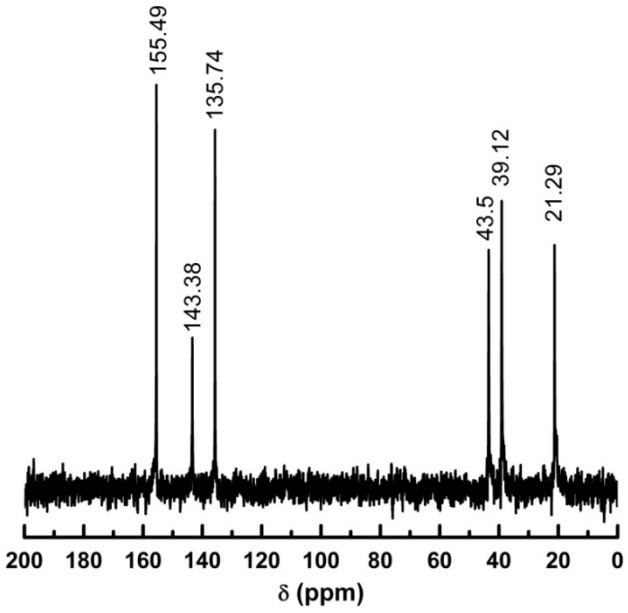

Figure S9. The ^{13}C NMR spectrum for the reaction mixture.

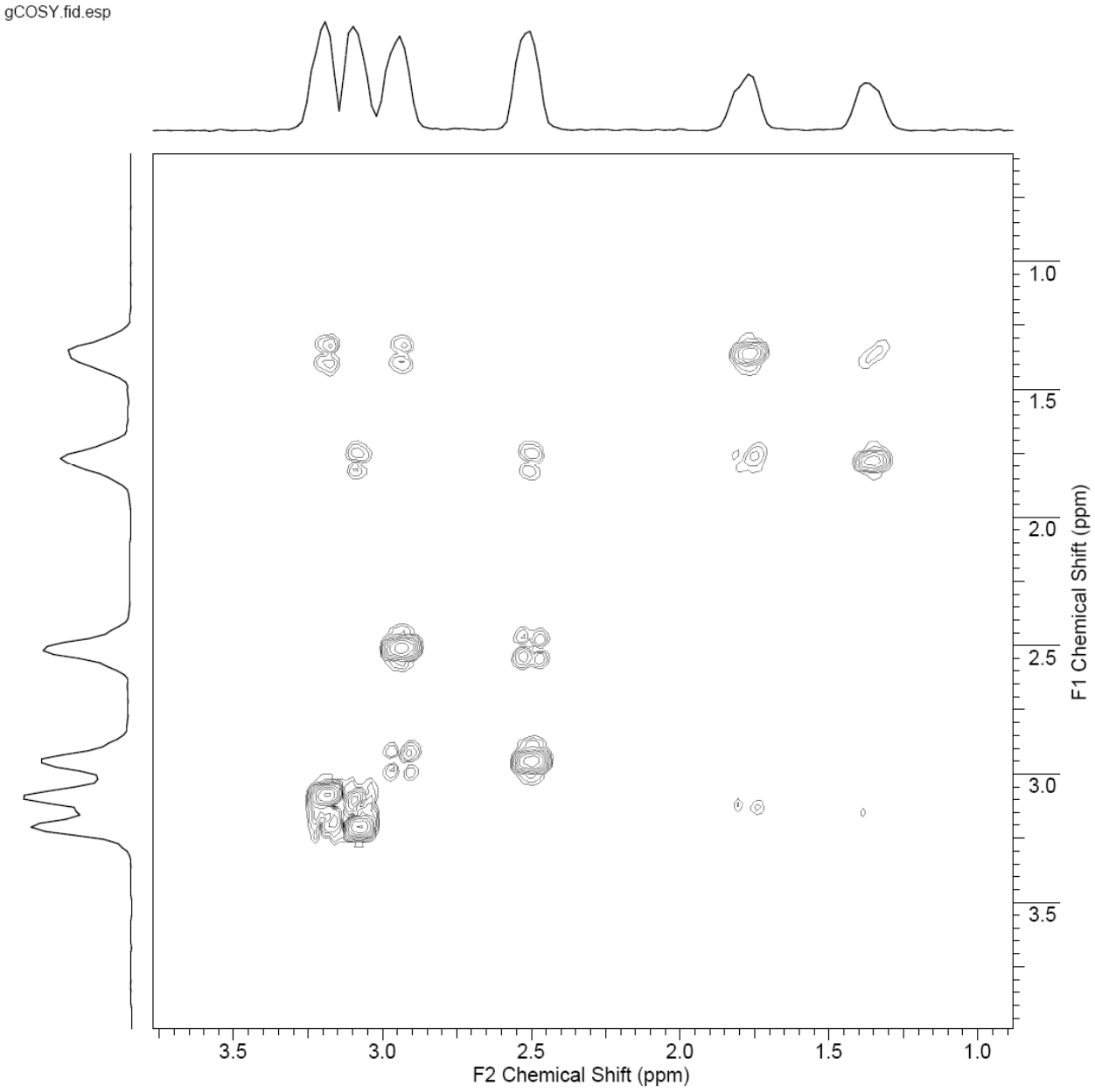

Figure S10. The ^{1}H-{^{1}H} gCOSY NMR spectrum for the reaction mixture.

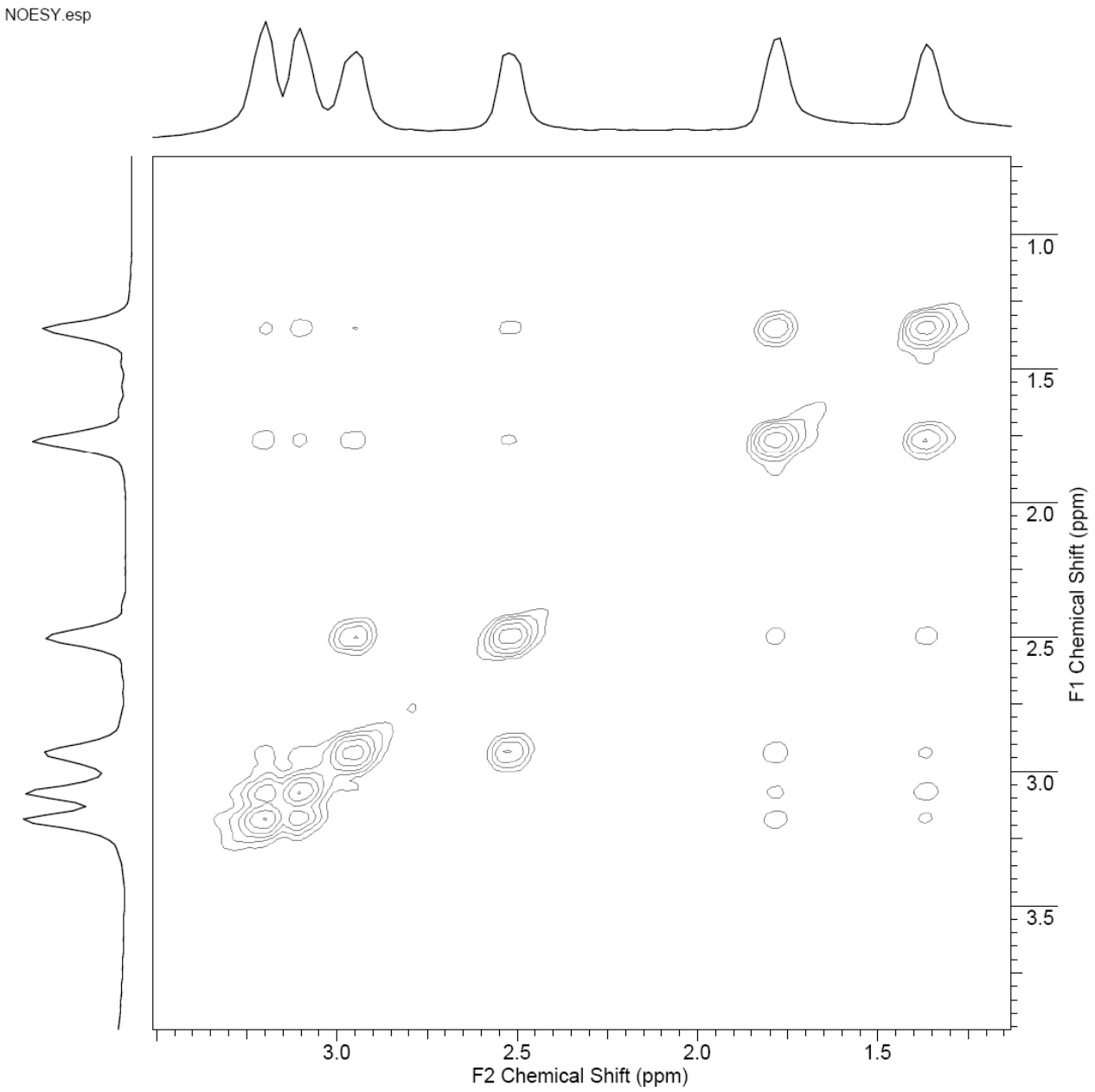

Figure S11 . ^{1}H-{^{1}H} NOESY NMR spectrum for the reaction mixture.

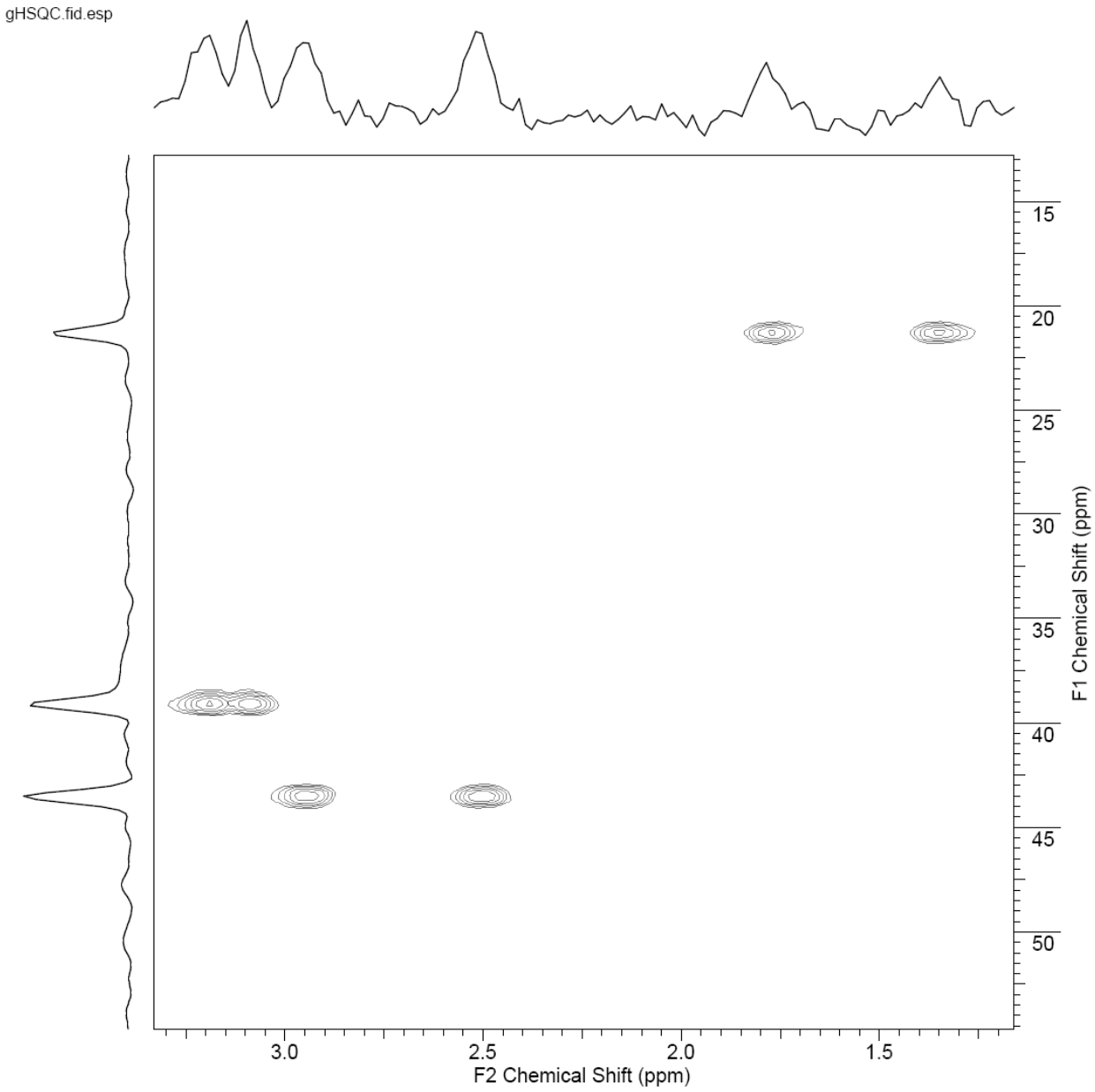

Figure S12. ^{1}H-{^{13}C} gHSQC NMR spectrum for the reaction mixture.

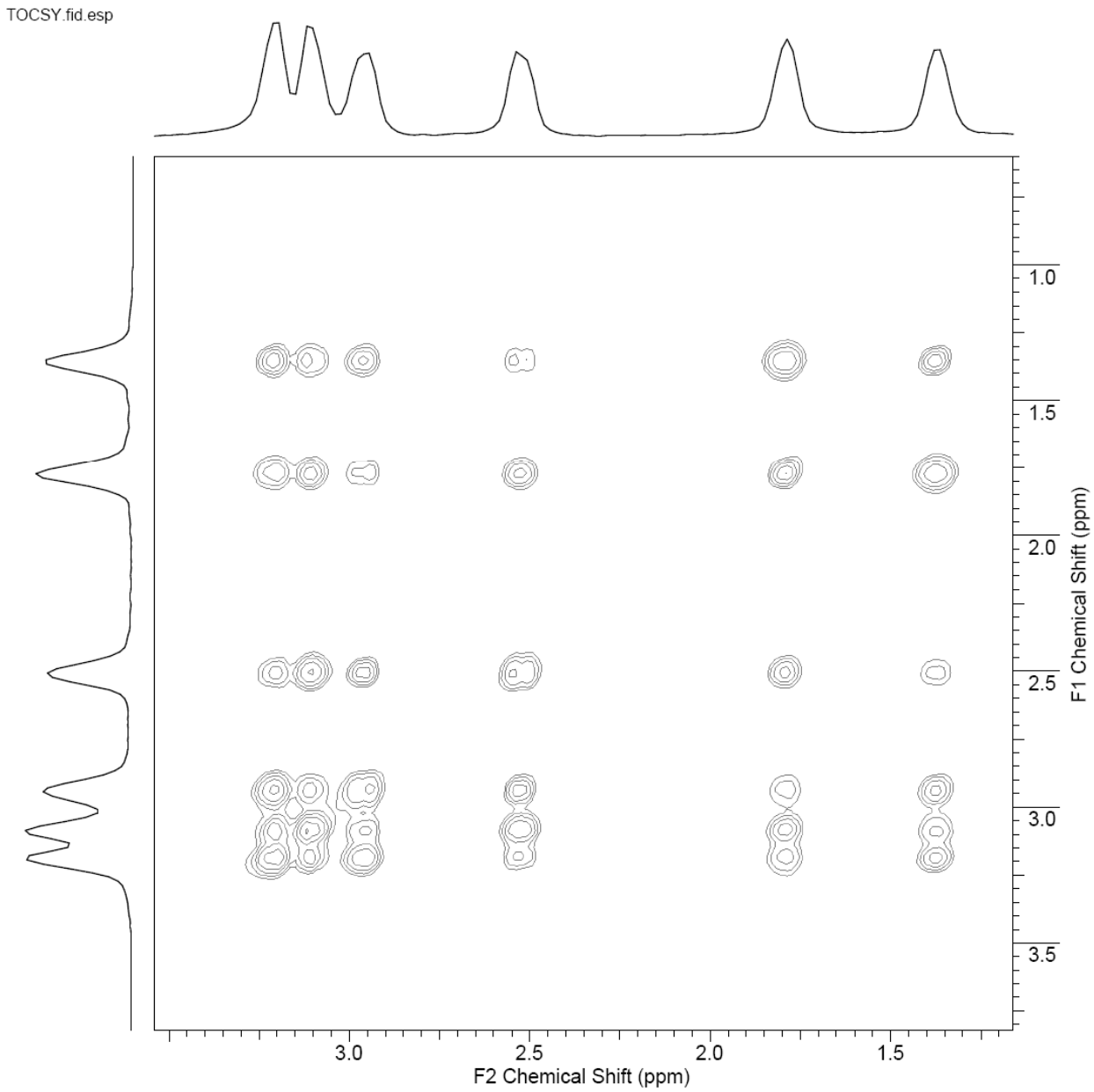

Figure S13. The ^{1}H-{^{1}H} TOCSY NMR spectrum for the reaction mixture.

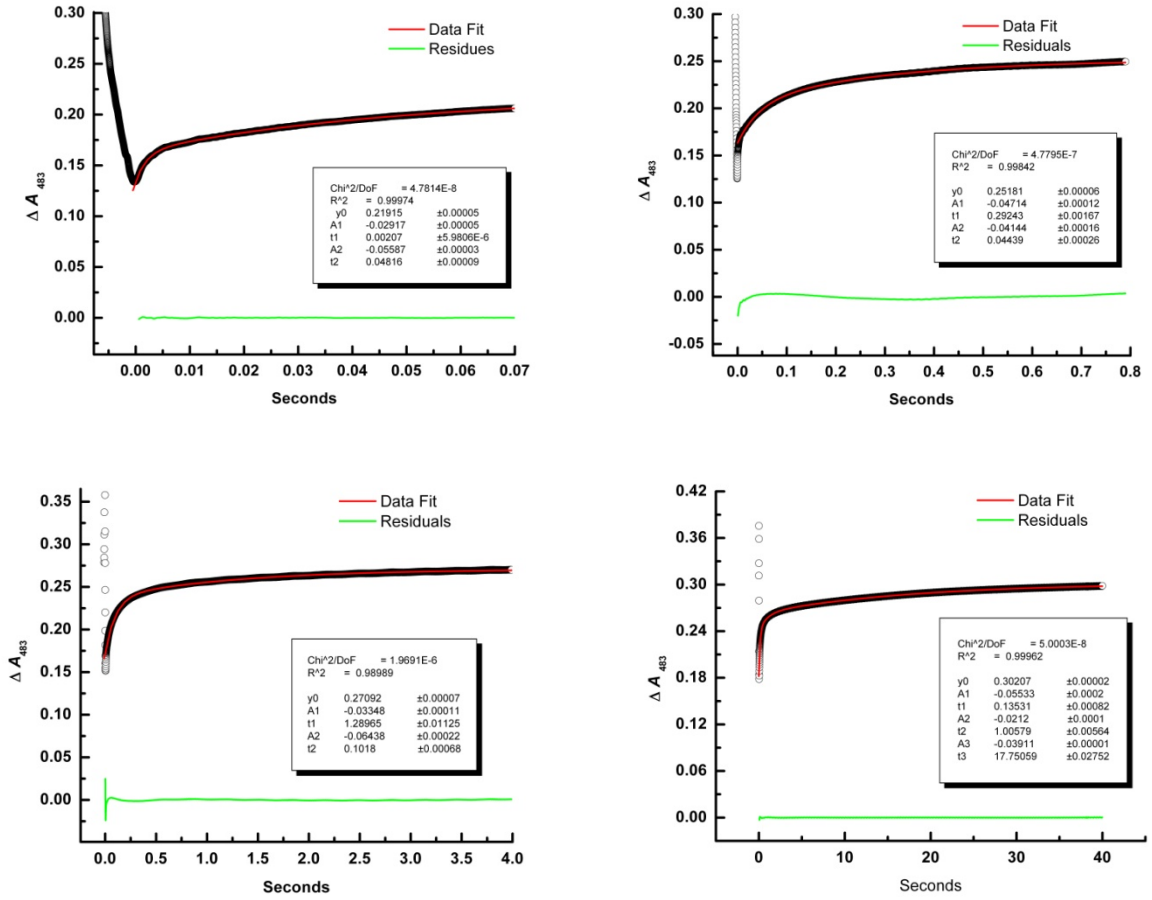

Figure S14. Stopped-flow kinetics of the 483nm absorption band for the complex.

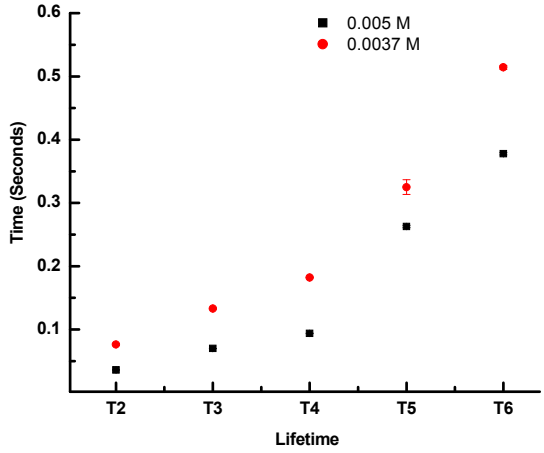

Figure S15. Concentration dependence of lifetime (**L1** concentration is indicated in the figure).

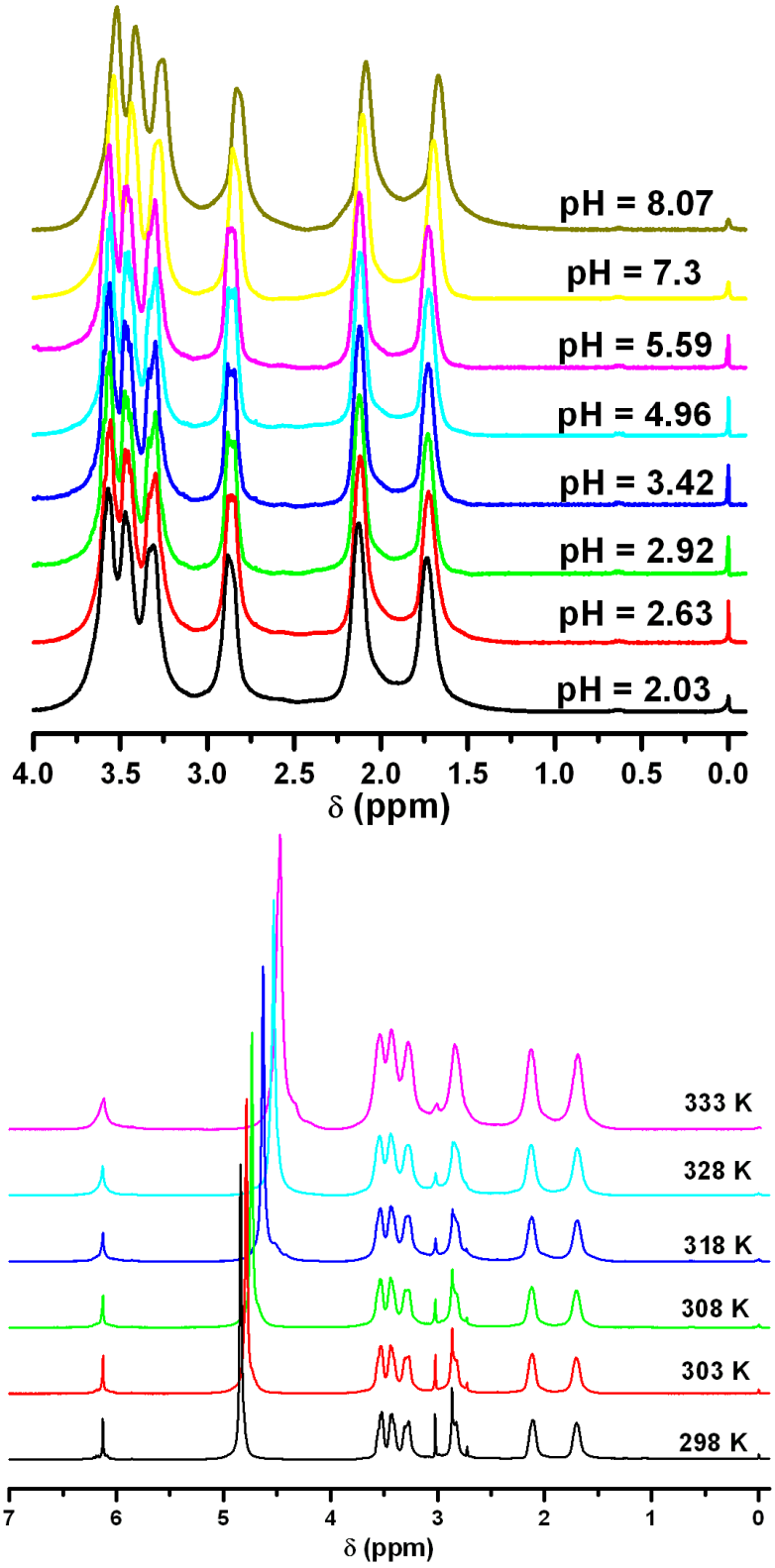

Figure S16. (Above) ^{1}H NMR spectra for the reaction mixture in D_2O at various apparent solution pH. Spectra acquired at 298 K and referenced to DSS at 0 ppm, (below) variable temperature ^{1}H NMR spectra for **1S** in D_2O, spectra are referenced to DSS as an internal standard at 0 ppm.

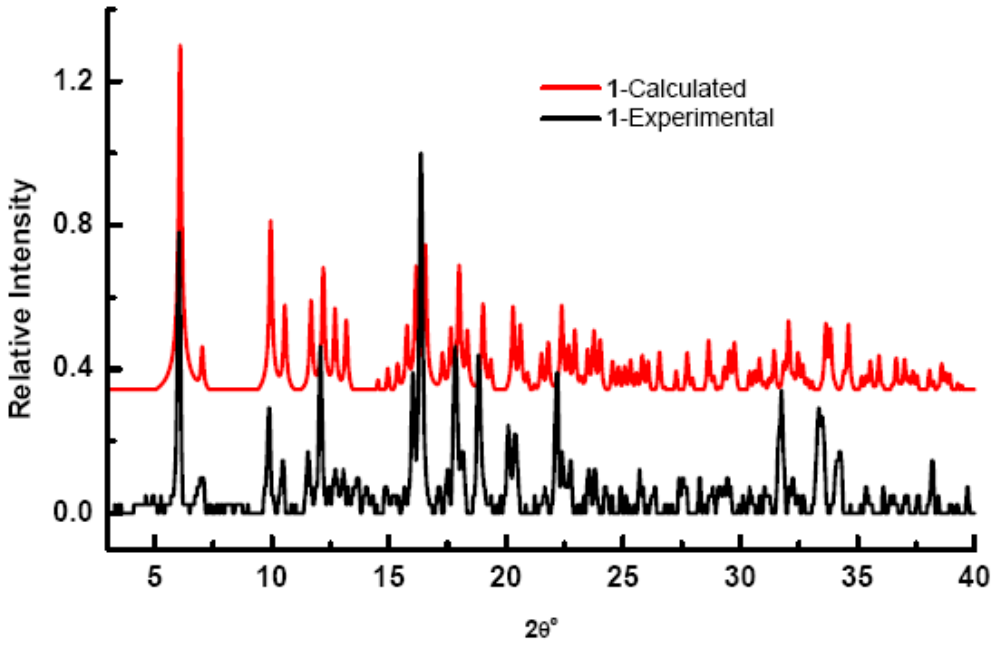

Figure S17. Calculated (red) and experimental (black) X-ray powder diffraction patterns for **1**.

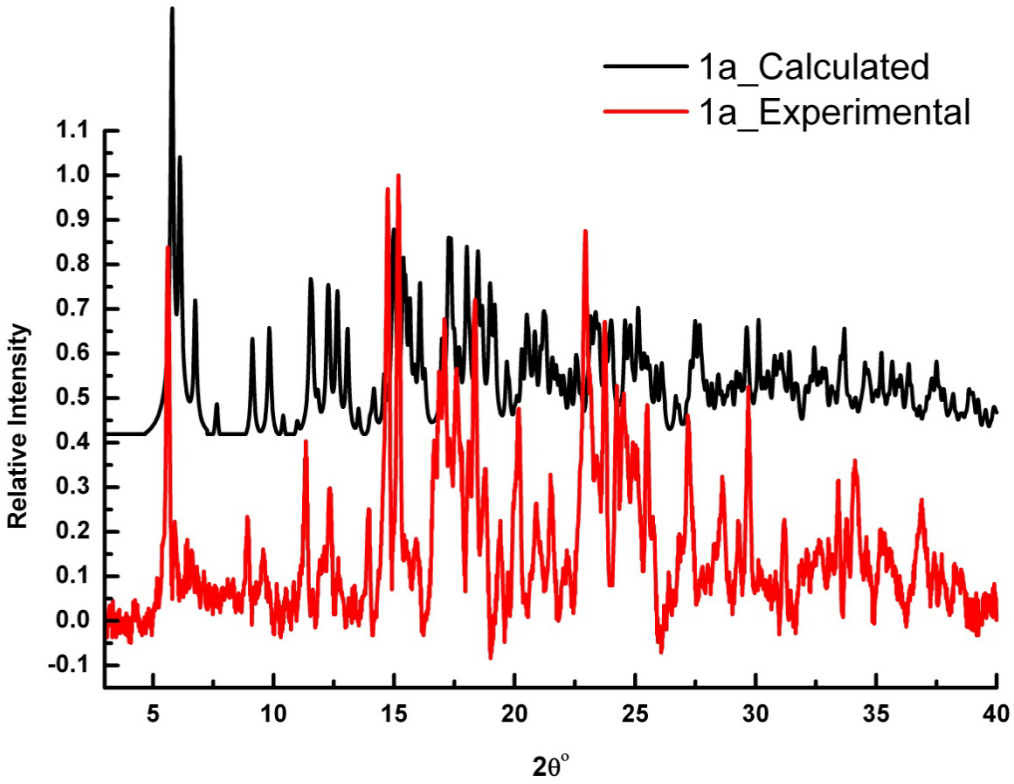

Figure S18. Calculated (red) and experimental (black) X-ray powder diffraction patterns for **1a**.

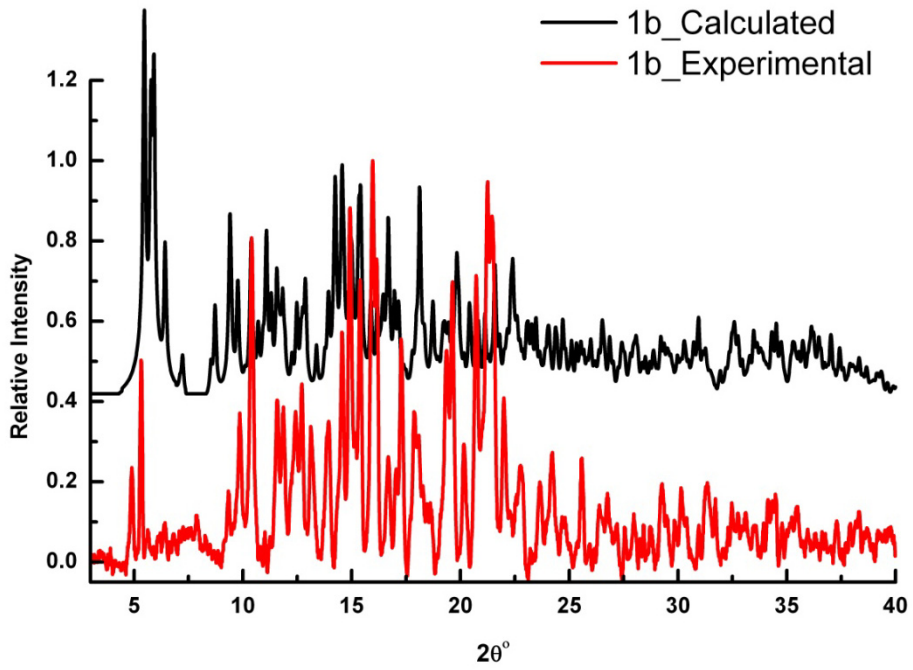

Figure S19. Calculated (red) and experimental (black) X-ray powder diffraction patterns for **1b**.

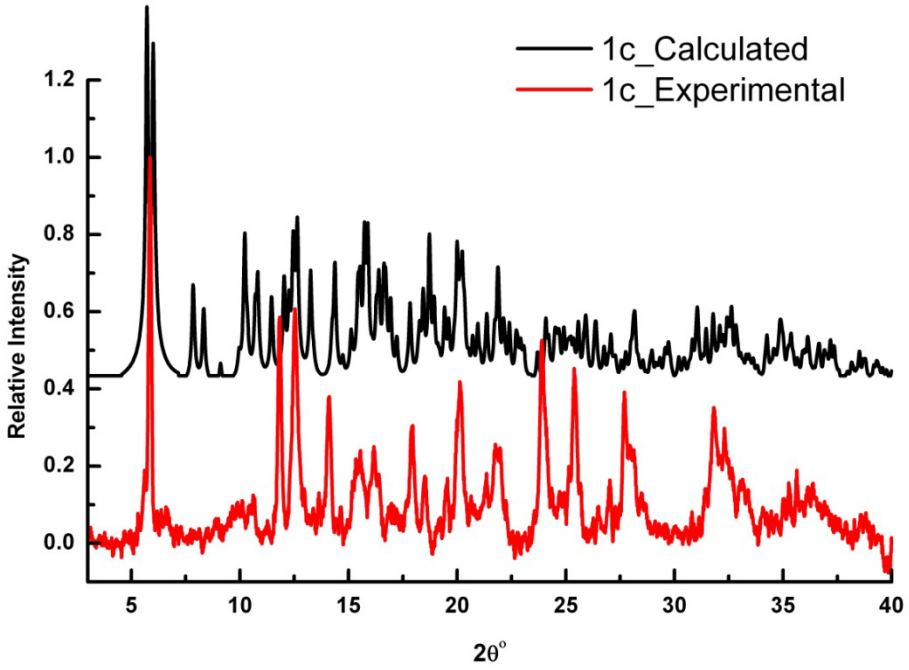

Figure S20. Calculated (red) and experimental (black) X-ray powder diffraction patterns for **1c**.

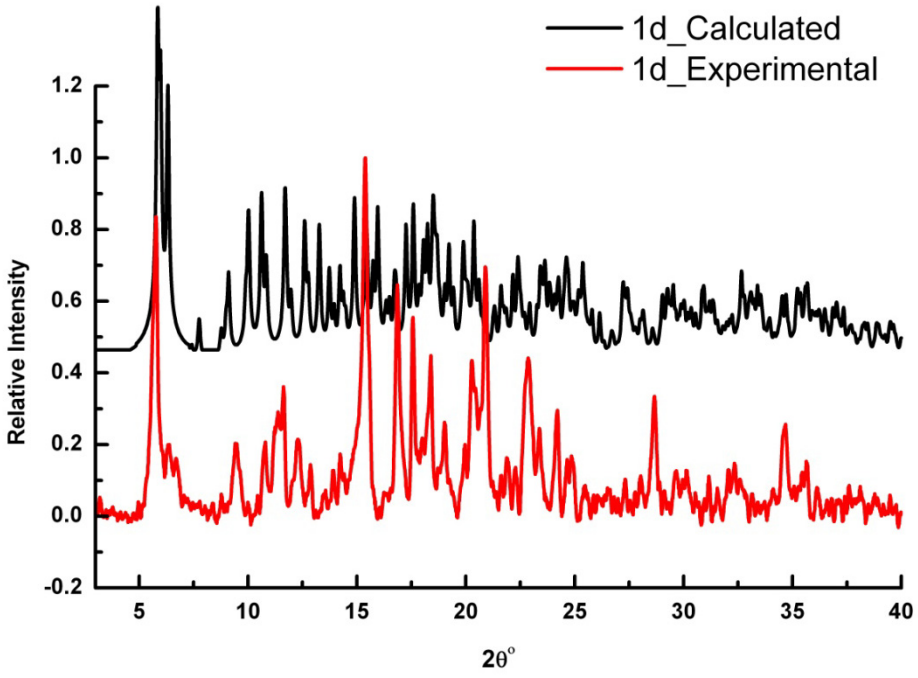

Figure S21. Calculated (red) and experimental (black) X-ray powder diffraction patterns for **1d**.

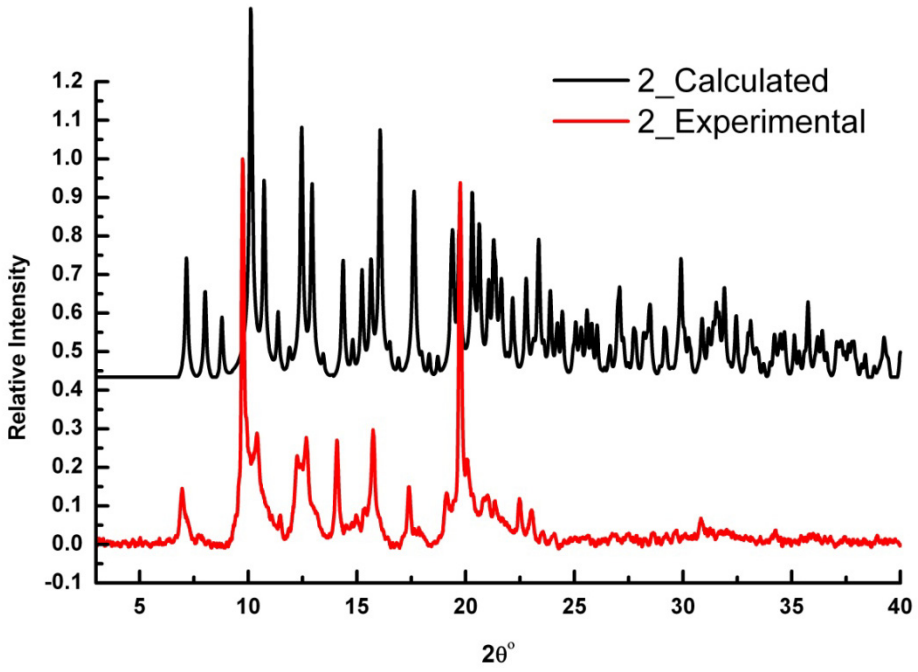

Figure S22. Calculated (red) and experimental (black) X-ray powder diffraction patterns for **2**.

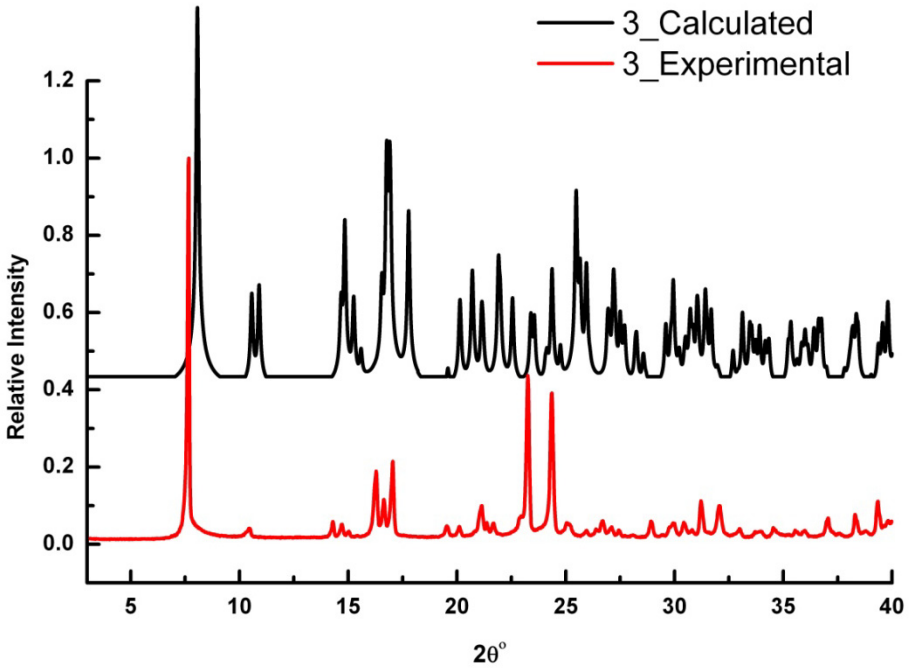

Figure S23. Calculated (red) and experimental (black) X-ray powder diffraction patterns for **3**.

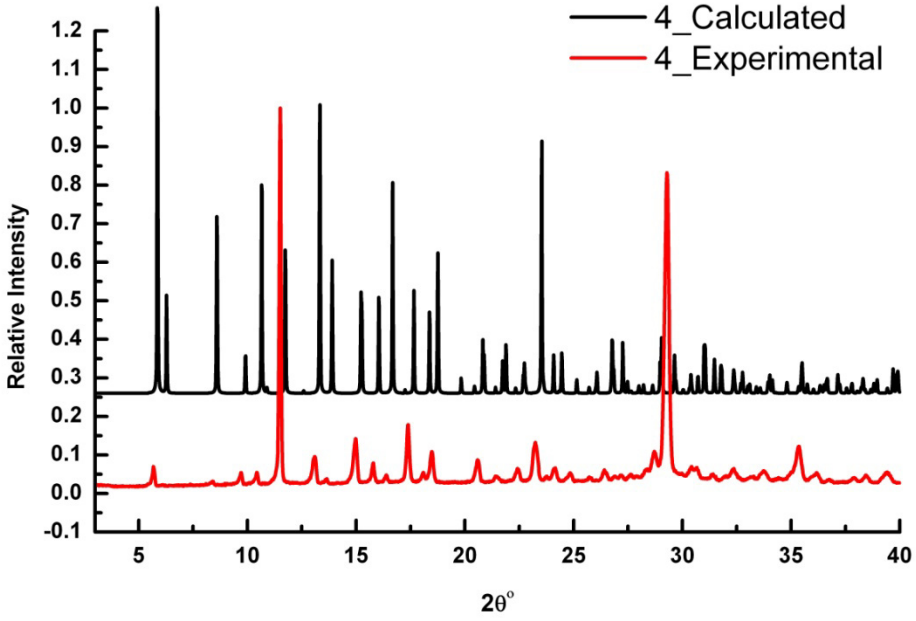

Figure S24. Calculated (red) and experimental (black) X-ray powder diffraction patterns for **4**.

References

1. Bruker-AXS (2001). SMART-V5.625. Data Collection Software. Madison, Wisconsin, USA.
2. Bruker-AXS (2001). SAINT-V6.28A. Data Reduction Software. Madison, Wisconsin, USA.
3. Sheldrick, G. M. (1996). SADABS. Program for Empirical Absorption Correction. University of Gottingen, Germany.
4. (a) Sheldrick, G. M. SHELXTL, v. 6.10; Bruker-AXS Madison, Wisconsin, USA. 2000. (b) Farrugia L. *J. Appl. Cryst.* **1999**, *32*, 837-838. (c) Sheldrick, G.M. *Acta Cryst*. **2008**, *A64*, 112-122. (d) Sheldrick, G.M. *Acta Cryst.* **1990**, *A46*, 467-473.
5. Gaussian 03, Revision C.02, M. J. Frisch, G. W. Trucks, H. B. Schlegel, G. E. Scuseria, M. A. Robb, J. R. Cheeseman, J. A. Montgomery, Jr., T. Vreven, K. N. Kudin, J. C. Burant, J. M. Millam, S. S. Iyengar, J. Tomasi, V. Barone, B. Mennucci, M. Cossi, G. Scalmani, N. Rega, G. A. Petersson, H. Nakatsuji, M. Hada, M. Ehara, K. Toyota, R. Fukuda, J. Hasegawa, M. Ishida, T. Nakajima, Y. Honda, O. Kitao, H. Nakai, M. Klene, X. Li, J. E. Knox, H. P. Hratchian, J. B. Cross, V. Bakken, C. Adamo, J. Jaramillo, R. Gomperts, R. E. Stratmann, O. Yazyev, A. J. Austin, R. Cammi, C. Pomelli, J. W. Ochterski, P. Y. Ayala, K. Morokuma, G. A. Voth, P. Salvador, J. J. Dannenberg, V. G. Zakrzewski, S. Dapprich, A. D. Daniels, M. C. Strain, O. Farkas, D. K. Malick, A. D. Rabuck, K. Raghavachari, J. B. Foresman, J. V. Ortiz, Q. Cui, A. G. Baboul, S. Clifford, J. Cioslowski, B. B. Stefanov, G. Liu, A. Liashenko, P. Piskorz, I. Komaromi, R. L. Martin, D. J. Fox, T. Keith, M. A. Al-Laham, C. Y. Peng, A. Nanayakkara, M. Challacombe, P. M. W. Gill, B. Johnson, W. Chen, M. W. Wong, C. Gonzalez, and J. A. Pople, Gaussian, Inc., Wallingford CT, 2004.
6. (a) A.D.Becke. *J.Chem.Phys*. **1993**, *98*, 5648-5642. (b) P.J.Stephens, F.J.Devlin, C.F.Chablowski, M.J.Frisch, *J.Phys.Chem*.**1994**, *98*, 11623-11627. (c) R.H.Hertwig, W.Koch, *Chem.Phys.Lett*.**1997**, *268*, 345-351.
7. (a) Dunning Jr., T. H.; Hay, P. J. "Methods of Electronic Structure Theory", Vol. 2, H. F. Schaefer III, ed., PLENUM PRESS (1977). (b) Hay, P. J.; Wadt, W. R. *J. Chem. Phys.* **1985**, *82*, 270.